ELSEVIER

Journal of Chromatography A, 709 (1995) 51–62

JOURNAL OF CHROMATOGRAPHY A

Electroosmosis in capillary zone electrophoresis with non-uniform zeta potential

Blahoslav Potoček[a], Bohuslav Gaš[a,*], Ernst Kenndler[b], Milan Štědrý[a]

[a]*Faculty of Science, Charles University, Albertov 2030, 128 40 Prague 2, Czech Republic*

[b]*Department of Analytical Chemistry, University of Vienna, Währinger Strasse 38, A1090 Vienna, Austria*

Abstract

The influence of the longitudinally non-uniform zeta potential on processes in capillary zone electrophoresis was studied. The velocity field of the electroosmotic flow in capillary tubes is modelled by the Navier–Stokes equations. Their stationary solution represents convective transport of a solute which is taken into account in the continuity equation for the concentration distribution. All equations are studied numerically. The results represent the time evolution of initial forms of sample peaks. These are presented in graphical form for several cases of zeta potentials which are either instructive or closely related to situations encountered in practice. It is shown that plug-like flow in the capillary cannot be expected and that a non-uniform zeta potential generally leads to significant dispersion of peaks.

1. Introduction

One of the most important phenomena accompanying the separation process in capillary zone electrophoresis (CZE) is the electroosmotic flow (EOF). This flow can be easily explained by invoking the electric double layer. Of all the possible reasons for its formation, the following two are worth mentioning: the specific adsorption of charged ionic species and protolysis of dissociable groups on the inner surface of the separation column. Since the net charge density ρ in the diffusion part of the double layer differs significantly from zero, an applied longitudinal electric field of strength E exerts the volume force $E\rho$ on the diffusion layer. As a consequence, the diffusion layer moves and owing to viscosity forces this movement is propagated to the rest of the liquid in the column.

In the description of the process, the electric potential Φ can be substituted for the net charge density ρ. The Poisson and Boltzmann equations provide relationships among ρ and Φ [1]. In this paper, it is the value of the potential Φ on the wall–liquid interface which will be used to characterize the process. This function is called the zeta potential and is usually denoted by ζ.

Many papers have dealt with the problem of EOF under the assumption that ζ does not depend on the coordinate running along the longitudinal axis of the capillary [2–7]. A conclusion drawn from above-mentioned papers is that EOF generally has little influence on the efficiency in CZE when the driving electroosmotic force is uniform along the column.

Cases in which any of the quantities involved, e.g., the zeta potential ζ or the longitudinal field

* Corresponding author.

0021-9673/95/$09.50
SSDI 0021-9673(95)00109-3

E, are supposed to vary along the axis of the capillary are treated only occasionally. However, there are various reasons for the assumption of an axially non-uniform zeta potential. These can be both intentional ones caused by a chemical treatment of the inner surface of the capillary and casual ones caused by a reaction and/or an adsorption of a solute [8] at the interface.

Anderson and Idol [9] have studied the stationary flow pattern in a capillary under the influence of a zeta potential, which is a periodic non-uniform function of the axial variable. As governing equations of the flow they have taken the Stokes equations, i.e., the Navier–Stokes equations in which convective terms are neglected. Relations for fluid velocity have been derived by means of Fourier series expansion and, moreover, an equation for the mean fluid velocity has been presented.

Chien and Helmer [10] have proposed a model to calculate the average electroosmotic velocity and the variance of sample peaks in field-amplified capillary electrophoresis, using a capillary column filled with two different concentrations of the same buffer. Thus, in their analysis, it is the field strength that appears to have a non-uniform distribution along the column. They realized that the radial velocity profile in parts with different concentrations has a parabolic shape and showed that the difference between the local electroosmotic velocities in both parts of the column and the mean velocity contributes to the dispersion of a solute in accordance with the Golay equation.

Towns and Regnier [11] have described how partial coverage of the inner surface of the column by adsorption of a protein leads to the mismatch between local and bulk electroosmotic velocity and consequently to a decrease in efficiency of separation.

Nowadays, attempts are made to use a radial electric potential across a capillary wall for a direct control of the zeta potential [12,13]. In the experimental equipment the radial electric potential is applied over a part but not the entire length of the column. Although experimental observations have been reported [14,15] indicating that the dispersion of peaks in this case does not satisfy the conclusions of Chien and Helmer, probably owing to surface conductivity, at least a gradual change in the axial distribution of the zeta potential [15] should be expected.

In this work, our aim was to study the migration of a solute in electrophoretic columns under the joint influence of the electrophoretic flux and convective transport through the electroosmotic flow caused by a longitudinally inhomogeneous zeta potential. A model is adopted in which the flow pattern in the column is found as a stationary solution of the Navier–Stokes equations with boundary conditions which depend on a given zeta potential. This stationary solution of the Navier–Stokes equations is found numerically. Another numerical procedure provides the concentration distribution of the solute as a function of two spatial variables and time. Results of simulations are given and commented on for three different distributions of zeta potential. It is concluded that the axially non-uniform zeta potential generally leads to dispersion of sample peaks and, sometimes, a noticeable radial distortion of the peak should be expected. In particular, the classical plug-like electroosmotic flow cannot be expected in cases where axial homogeneity of some quantities no longer holds.

2. Theory

We shall deal with a capillary column of radius a and finite length L. It will be assumed that $L \gg a$ and that all flows and fluxes and also the concentration distribution will be rotationally symmetrical.

2.1. Velocity field in the column

The velocity vector, $\vec{v}$, is equal to a two-dimensional vector (v_x, v_r), which consists of v_x, the axial, and v_r, the radial velocity component. Each component of the velocity vector depends on the axial coordinate x, the radial coordinate r and time t. The governing equations for the velocity $\vec{v}$ are the Navier–Stokes equations in which, with a view to rotational symmetry of the process, cylindrical variables will be used.

As the fluid is viscous, the boundary condition on the wall–liquid interface should be that the velocity is equal to zero and the volume force $E\rho$, from which the EOF stems, should occur in the Navier–Stokes equations. In this paper, for simplicity the fluid velocity on the column wall will be set to equal the electroosmotic plug velocity determined by the Helmholtz–Smoluchowski equation and, consequently, the volume force $E\rho$ does not appear in the equations governing the flow. This approximation was also used by other workers [9–11,16] and can be well accepted in most real instances when the thickness of the diffusion layer is much less then the inner diameter of the capillary column. Thus, the apparent electroosmotic velocity $v(x)$ at a point at the column wall with longitudinal coordinate x will be

$$v(x) = \frac{-\varepsilon E}{\eta}\,\zeta(x) \tag{1}$$

where ε is the permitivity of the liquid, E is the driving electric field strength, $\zeta(x)$ is the zeta potential, dependent on the axial x coordinate, and η is the dynamic viscosity of the liquid. In this paper it is further assumed for simplicity that the driving electric field is a constant vector parallel to the axis of the capillary.

The acceptance of the approximation used, Eq. 1, is well supported by Tikhomolova [6], who analytically calculated the time development of the electroosmotic velocity profile in the cylindrical column. Her results show that the velocity at the inner edge of the diffusion layer acquires the Helmholtz–Smoluchowski value $-\varepsilon E\zeta/\eta$ in a very short time even when the rest of the liquid is still not moving.

As the double layer is neglected, it is possible to express the boundary condition on the capillary wall for the axial velocity component in the form

$$v_x(x, a, t) = v(x) \tag{2}$$

where $v(x)$ is given by Eq. 1.

The velocity field and the function $p = p(x, r, t)$, describing pressure, satisfy the Navier–Stokes equations for incompressible fluid, which are considered in the domain $x \in \langle 0, L\rangle$, $r \in \langle 0, a\rangle$, $t \in \langle 0, \infty)$ and can be be given in the following form [17]:

$$\frac{\partial v_x}{\partial t} + v_x\frac{\partial v_x}{\partial x} + v_r\cdot\frac{\partial v_x}{\partial r} = \nu\left[\frac{\partial^2 v_x}{\partial x^2} + \frac{1}{r}\cdot\frac{\partial}{\partial r}\left(r\cdot\frac{\partial v_x}{\partial r}\right)\right] - \frac{1}{\rho_M}\cdot\frac{\partial p}{\partial x} \tag{3}$$

$$\frac{\partial v_r}{\partial t} + v_x\frac{\partial v_r}{\partial x} + v_r\frac{\partial v_r}{\partial r} = \nu\left[\frac{\partial^2 v_r}{\partial x^2} + \frac{1}{r}\cdot\frac{\partial}{\partial r}\left(r\frac{\partial v_r}{\partial r}\right) - \frac{v_r}{r^2}\right] - \frac{1}{\rho_M}\cdot\frac{\partial p}{\partial r} \tag{4}$$

$$\frac{\partial v_x}{\partial x} + \frac{1}{r}\cdot\frac{\partial}{\partial r}(rv_r) = 0 \tag{5}$$

where $\nu \equiv \eta/\rho_M$ is the kinematic viscosity and ρ_M is the mass density of the liquid. It will be assumed that the fluid is at rest at time $t = 0$, and therefore

$$v_x(x, r, 0) = 0\,, \quad v_r(x, r, 0) = 0 \tag{6}$$

On the capillary wall, the axial velocity is prescribed and the radial velocity must be equal to zero, i.e.

$$v_x(x, a, t) = v(x)\,, \quad v_r(x, a, t) = 0 \tag{7}$$

On the axis of the capillary, the components of the velocity satisfy these geometrical conditions:

$$\frac{\partial v_x}{\partial r}(x, 0, t) = 0\,, \quad v_r(x, 0, t) = 0 \tag{8}$$

It is assumed that both ends of the capillary are under constant pressure and, moreover, there is no difference between these pressures, i.e.,

$$p(0, r, t) = p_L\,, \quad p(L, r, t) = p_R \tag{9}$$

where p_L and p_R are constants for which $p_L = p_R$. If all significant changes occur in the area far from both ends of the capillary, it is acceptable to formulate the boundary conditions at the ends in the form

$$\frac{\partial v_x}{\partial x}(0, r, t) = 0\,, \quad v_r(0, r, t) = 0 \tag{10}$$

$$\frac{\partial v_x}{\partial x}(L, r, t) = 0\,, \quad v_r(L, r, t) = 0 \tag{11}$$

The second and third terms in Eqs. 3 and 4 are

convective terms which bring non-linearity into the Navier–Stokes equations. The Reynolds number Re, used to assess the significance of the convective terms, is defined for the case of flow in a cylindrical tube as $Re = av_0\rho_M/\eta$, where v_0 is a characteristic velocity. The convective terms could be neglected if $Re \ll 1$. Under the conditions that are typical of EOF in CZE, $v_0 = 1$ mm s^{-1}, $a \approx 100$ μm, $\rho_M = 1000$ kg m^{-3} and $\eta = 0.001$ Pa s, so $Re \approx 0.1$. This means that the convective terms might play a certain role in the capillary flow in CZE and were taken into account by using the Navier–Stokes equations.

It is obvious that the solution of the described system of equations depends on the function $v(x)$. With time increasing, this solution converges to a time-independent solution. A numerical procedure will be used to obtain an approximation to this stationary velocity field.

2.2. Concentration distribution

Once the velocity field is known, the concentration distribution of a solute, $c(x, r, t)$, can be calculated by solving the continuity equation

$$\frac{\partial c}{\partial t} = D\left[\frac{\partial^2 c}{\partial x^2} + \frac{1}{r}\cdot\frac{\partial}{\partial r}\left(r\cdot\frac{\partial c}{\partial r}\right)\right] - v_x\cdot\frac{\partial c}{\partial x} - v_r\cdot\frac{\partial c}{\partial r} - \mathrm{sgn}(z)\frac{\partial(cuE)}{\partial x} \quad (12)$$

with the initial condition

$$c(x, r, 0) = c_0(x, r) \quad (13)$$

and the boundary conditions consisting of a condition on the capillary wall given by

$$\frac{\partial c}{\partial r}(x, a, t) = 0 \quad (14)$$

a geometrical condition on the capillary axis given by

$$\frac{\partial c}{\partial r}(x, 0, t) = 0 \quad (15)$$

and the following conditions in the ends of the capillary:

$$c(0, r, t) = c_L\,, \quad c(L, r, t) = c_R \quad (16)$$

Here, D is the diffusion coefficient, u is the electrophoretic mobility of the solute and z is its charge number. It is seen that the continuity Eq. 12 takes several fluxes into account, namely the diffusional flux (the first term on the right-hand side), the flow in the electroosmotic velocity field (the second and third terms) and the electrophoretic flux (the fourth term). The electrophoretic flux is the movement of a solute with the velocity $v_{ep} = \mathrm{sgn}(z)uE$ only in the axial direction due to the Coulombic force acting on possibly charged particles of the solute.

It will be assumed that

$$c_L = c_R = 0 \quad (17)$$

The initial concentration distribution described by function $c_0(x, r)$ must satisfy all boundary conditions. Since in this paper the function $c_0(x, r)$ will have the form $c_0(x)$, i.e., it does not depend on the radial variable r, we shall assume that

$$c_0(0) = c_0(L) = 0 \quad (18)$$

In problems of movement of a solute along a tube, the mean radial concentration c_m is a useful quantity:

$$c_m(x, t) = \frac{2}{a^2}\int_0^a c(x, r, t) r\,\mathrm{d}r \quad (19)$$

The dispersion $\sigma^2(t)$ will be defined in analogy with the dispersion of c_m in the unbounded capillary by

$$\sigma^2(t) = \frac{1}{c_{tot}(t)}\int_0^L c_m(x, t)[x - \mu(t)]^2\,\mathrm{d}x \quad (20)$$

where $\mu(t)$, the mean x-coordinate of the solute, is

$$\mu(t) = \frac{1}{c_{tot}(t)}\int_0^L c_m(x, t) x\,\mathrm{d}x \quad (21)$$

and

$$c_{tot}(t) = \int_0^L c_m(x, t)\,\mathrm{d}x \quad (22)$$

The mean velocity of the convective flow in the capillary tube, v_m, is defined by

$$v_m(t) = \frac{2}{a^2}\int_0^a v_x(x, r, t) r \, dr \quad (23)$$

This value, due to the condition of incompressibility, does not depend on the variable x. With the time increasing, $v_m(t)$ converges to a stationary value. This value will be referred to as the stationary mean velocity. In cases when both convective flow and electrophoretic flux act together, the solute moves at the velocity $v_m + v_{ep}$.

There have been several studies of the time development of a solute concentration (or, at least, dispersion of a solute) under the influence of various types of flows in tubes. A stationary velocity field with parabolic profile has been considered [18–22] and the electroosmotic velocity profile encountered in stationary EOF with zeta potential uniform along the capillary tube has been investigated [3,4,7].

Using the Stokes equations, Anderson and Idol [9] derived that the stationary mean velocity, v_m, attains the value given by

$$v_m = \frac{1}{L}\int_0^L v(x)\, dx \quad (24)$$

For the sake of completeness, it is shown in the Appendix how Eq. 24 can be obtained through a simple computation with the Stokes equations. If the Navier–Stokes equations are used, Eq. 24 is not exactly valid. However, only a small deviation of the stationary mean velocity from the value given by Eq. 24 can be expected. This is what has been confirmed by numerical simulations.

3. Methods of solution

The Navier–Stokes Eqs. 3–5 were transformed into a system of partial differential equations for a pair of functions, ψ and ξ [23]. The stream function ψ, provides the velocity components through the equations

$$v_x = \frac{1}{r}\cdot\frac{\partial\psi}{\partial r}, \quad v_r = -\frac{1}{r}\cdot\frac{\partial\psi}{\partial x} \quad (25)$$

The vorticity of the velocity field, ξ, is given by

$$\xi = \frac{\partial v_r}{\partial x} - \frac{\partial v_x}{\partial r} \quad (26)$$

The functions ξ and ψ satisfy the following system:

$$\frac{\partial\xi}{\partial t} + v_x\cdot\frac{\partial\xi}{\partial x} + v_r\cdot\frac{\partial\xi}{\partial r} - \frac{v_r\xi}{r} = \nu\left[\frac{\partial^2\xi}{\partial x^2} + \frac{1}{r}\cdot\frac{\partial}{\partial r}\left(r\cdot\frac{\partial\xi}{\partial r}\right) - \frac{\xi}{r^2}\right] \quad (27)$$

$$\frac{\partial^2\psi}{\partial x^2} + r\cdot\frac{\partial}{\partial r}\left(\frac{1}{r}\cdot\frac{\partial\psi}{\partial r}\right) = -r\xi \quad (28)$$

The conditions to which the function ξ is subject consist of an initial condition

$$\xi(x, r, 0) = 0 \quad (29)$$

and the boundary conditions

$$\xi(x, a, t) = -\frac{\partial}{\partial r}\left(\frac{1}{r}\cdot\frac{\partial\psi}{\partial r}\right)(x, a, t), \quad \xi(x, 0, t) = 0 \quad (30)$$

$$\frac{\partial\xi}{\partial x}(0, r, t) = 0, \quad \frac{\partial\xi}{\partial x}(L, r, t) = 0 \quad (31)$$

The boundary conditions for ψ are

$$\psi(x, a, t) = \chi(t), \quad \psi(x, 0, t) = 0 \quad (32)$$

$$\frac{\partial\psi}{\partial x}(0, r, t) = 0, \quad \frac{\partial\psi}{\partial x}(L, r, t) = 0 \quad (33)$$

where the function $\chi(t)$ is a function which depends on only one variable, t, and satisfies the relationship

$$L\cdot\frac{d\chi}{dt}(t) = -\nu a\int_0^L \xi(x, a, t)\, dt - \int_0^L\int_0^a\left(v_x\cdot\frac{\partial v_x}{\partial x} + v_r\cdot\frac{\partial v_x}{\partial r}\right) r \, dr \, dx \quad (34)$$

Finite difference methods were used to solve the Navier–Stokes equations and the parabolic equation for the concentration of a solute. With a Reynolds number of moderate value, we were able to apply all methods [17,23,24] in a straightforward and standard manner.

4. Results and discussion

The mathematical model described above enables one to calculate a velocity field and peak shapes of a solute for arbitrary axial distributions of the zeta potential. We shall discuss several instances of such forms of the zeta potential which are either instructive or closely related to situations encountered in practice. In all simulations, the liquid is meant to be water with dynamic viscosity $\eta = 0.001$ Pa s and mass density density $\rho_M = 1000$ kg m^{-3}.

4.1. Half-covered capillary column

A capillary column is considered in which the right half is covered by a deactivation layer. The consequence is that, except for a transition region around the centre of the capillary, the zeta potential is constant and equals zero in the right part of the capillary and a non-zero value in the left-hand side of the capillary.

Various widths of the transition region between the covered and uncovered parts of the capillary are modelled by taking three functions $\zeta(x)$ with various steepness in the transient region. These functions, playing the role of the input boundary conditions, are depicted in Fig. 1a as curves 1, 2 and 3. All these functions are such that the local electroosmotic velocity generated by the value of the zeta potential at the left end of the capillary is 1 mm s^{-1} and that at the right end is zero.

The corresponding stationary velocity fields obtained by solving Eqs. 3–11 for a capillary with an inner diameter of 100 μm ($a = 50 \cdot 10^{-6}$ m) are shown in Fig. 1b for all three cases of $v(x)$. In this and all analogous figures the radial size of the capillary is considerably enlarged and so the radial velocity component has also been magnified in the same ratio. The vectors of the velocity are depicted as "weathercocks" streaming in the flow. The lengths of lines attached to the depicted points are proportional to the magnitude of the velocity. It is seen that a radial component of the velocity appears mainly in the transient region. At a distance a few diameters from the transient region the radial flows are negligible and the axial component of the velocity field has an almost parabolic profile. In the left part of the column the axial component of the velocity is maximum at the column wall and nearly zero on the axis whereas in the right part of the column the situation is the opposite, i.e. the maximum velocity is on the axis and zero at the wall.

We shall investigate the time development of a Gaussian peak of a solute with a diffusion coefficient $1 \cdot 10^{-10}$ m^2 s^{-1}, the centre of which is at a position $x = 8$ mm in the capillary tube, its initial variance is $\sigma_i^2 = 2.5 \cdot 10^{-7}$ m^2 and its concentration in the maximum is 4 mol m^{-3} (4 mM). The initial axial distribution of the solute is depicted in Fig. 1a. The initial condition, Eq. 13, is

$$c_0(x, r) = 4 \exp\left[-\frac{(x - 0.008)^2}{2 \cdot 2.5 \cdot 10^{-7}} \right] \tag{35}$$

In fact, this function satisfies the boundary conditions given by Eqs. 18 only approximately, but the small difference can be neglected. It will be assumed for simplicity that the solute has no electric charge, i.e., $u = 0$ and consequently $v_{ep} = 0$ in this case.

Numerically solving Eqs. 12–18 gives the concentration distribution $c(x, r, t)$. The mean velocity v_m calculated with the aid of Eq. 24 is 0.5 mm s^{-1}, whereas v_m obtained from the movement of the simulated peak of the solute is about 0.49 mm s^{-1} for all three cases. This indicates a slight influence of convective terms in the Navier–Stokes equations.

The time-dependent variance of the solute calculated by Eq. 20 is depicted in Fig. 1c for all three cases of v. The mean velocity v_m is almost the same in all three cases but the corresponding dispersion of a passing solute peak depends considerably on the course of the function v. The less steep the function $v(x)$ in the transient region, the smaller is the resulting value of the solute variance. In the situation described, the main cause of the peak dispersion is due to the parabolic profile of the axial velocity component, which dominates over the radial component. In accordance with Chien and Helmer's considera-

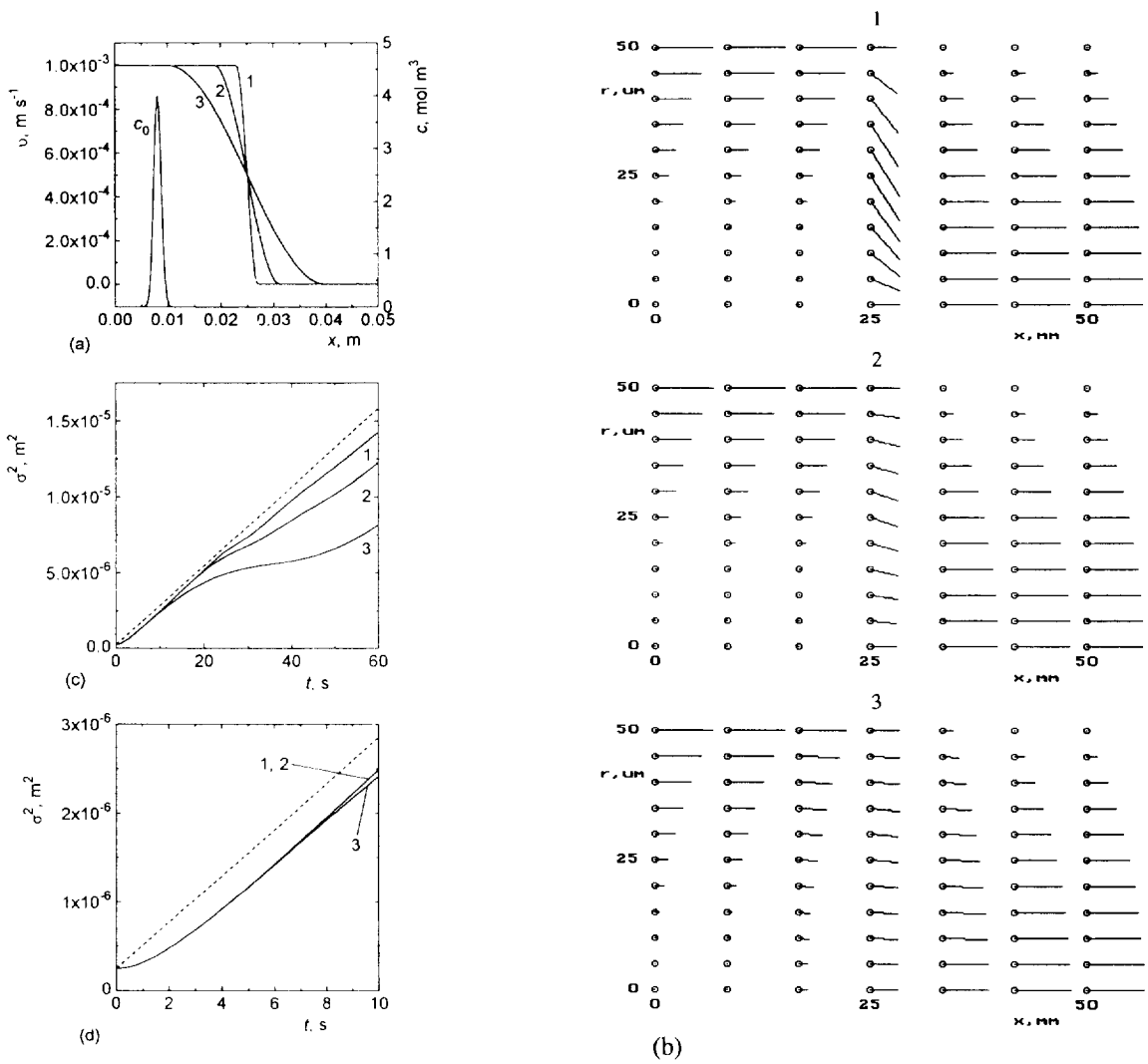

Fig. 1. Simulation of the stationary velocity field in a half-covered capillary column. Diffusion coefficient D, $1 \cdot 10^{-10}$ m^2 s^{-1}; radius of column a, $50 \cdot 10^{-6}$ m; length of column L, 0.05 m; electrophoretic velocity v_{ep}, 0. c_0 = Initial condition, Eq. 35. 1–3 = Three different cases corresponding to three profiles of the electroosmotic velocity $v(x)$ at the column wall. Dashed line = time-dependent variance of convective diffusion in a laminar parabolic flow with the velocity of 0.5 mm s^{-1}. (a) Initial condition and boundary conditions; (b) velocity fields; (c) and (d) simulated time-dependent variance.

tions [10], it is the difference between the "local" and mean velocity which contributes mainly to the peak broadening. The term "local" velocity means the velocity v at the site of the peak, but it should be realized that the peak has a certain axial width, so there is no uniqueness in the determination of the local velocity.

In the parts of the column outside the transient region, the difference between the velocity v and the mean velocity given by Eq. 24 is $v_{dif} = \pm 0.5$ mm s^{-1}. For comparison, a dashed line with the slope $v_{dif}^2 a^2/24D$ is drawn in Fig. 1c and d, which corresponds to a laminar parabolic flow with a velocity of 0.5 mm s^{-1}.

Additionally, it is worth noting that the simulated curves start with almost zero slope at time $t = 0$, but after a few seconds the slope stabilizes to a value which is near to that predicted by

$v_{diff}^2 a^2/24D$. The part of Fig. 1c around $t = 0$ is enlarged and shown in Fig. 1d. This result can be viewed in the context of the conclusions in the paper by Gill and Sankarasubramanian [22]. For the case of unsteady convective diffusion in the laminar flow, they calculated that the slope of variance stabilizes at time $t \approx 0.2a^2/D$. In our case this value is 5 s, which corresponds well with the simulated case.

A solute peak exhibits interesting changes in its radial and axial profiles when passing through the transient region. These changes are especially profound when, roughly, the velocity of the axial movement of the solute is comparable to the speed of the radial diffusion flux. In typical CZE conditions this can happen in rather thick columns or in the case of a low diffusion coefficient of the solute. Fig. 2a shows both the axial and radial profiles of an analyte with diffusion coefficient $5 \cdot 10^{-11}$ m^2 s^{-1} (this would correspond, e.g., to the diffusion coefficient of conalbumin) in a column of 150 μm I.D. passing through the transient region depicted as curve 1 in Fig. 1a. The curves in Fig. 2a come from the solutions to the Eqs. 12–18. The mean radial concentration profile c_m at various times is given by the thick line. In Fig. 2b a time record is depicted which would be recorded by a detector located at a position just behind the transient region. In spite of peculiar changes in the axial and radical peak profiles, the time record is only a simple tailing profile.

4.2. Partly-covered capillary column

In this example, a segment of the capillary column a part of which, say one third or two thirds is covered by a layer hindering the formation of a non-zero zeta potential. Fig. 3a illustrates the corresponding functions $v(x)$, i.e., the distribution of the electroosmotic velocity along the column. Although this case is a slight generalization of the previous half-and-half case, the flow pattern of the velocity field is different because significant vortices in the flow may appear. Fig. 3b shows a plot of the calculated velocity fields in both cases. The "weathercocks" directing to the left indicate the appearance of vortices. Nevertheless, it should be realized that the mean flow of the liquid directs to the right in both cases with a mean velocity of about 1/3 or 2/3 mm s^{-1}, respectively.

4.3. Partly uncovered capillary column at the detector position

Capillary columns with an inner coating suppressing the EOF are often used. The columns are also always coated from the outer side by a polymer coating. As the outer polymer coating is UV absorbing, it is necessary to remove it at the site of the UV absorption detector. This is often done by means of a flame which burns off the polymer coating in the region of the capillary where the detector will be located. However, the inner coating will also be destroyed by this procedure. Such a situation can cause severe problems from the point of dispersion of the passing solute due to the EOF occurring in the uncovered region. This situation is stimulated in a 5-cm segment of a covered capillary column, 1 cm of which is uncovered. The detector is situated in the middle of the uncovered part. Fig. 4a shows the function $v(x)$ and Fig. 4b the calculated velocity field in the capillary of 100 μm I.D. The closed vortices in the velocity field are evident.

An initial Gaussian peak of a solute with a diffusion coefficient of $2 \cdot 10^{-10}$ m^2 s^{-1} will be assumed to move in the column. The centre of its initial position will again be at $x = 8$ mm and its initial variance will be $\sigma_i = 2.5 \cdot 10^{-7}$ m^2. The mean velocity v_m of the flow in the capillary according to Eq. 24 is 0.2 mm s^{-1}. Now it is assumed that the solute has an electric charge causing its migration in the electric field with an electrophoretic velocity $v_{ep} = 0.5$ mm s^{-1}. The total velocity of the movement of the solute in the column will therefore be $v_m + v_{ep} = 0.7$ mm s^{-1}. Fig. 4c shows a plot of σ^2 against time. There is apparently a significant total increase in the solute dispersion while the peak is passing through the uncovered region of the capillary. However, rather than knowing the dispersion changing with time, one may be interested in the

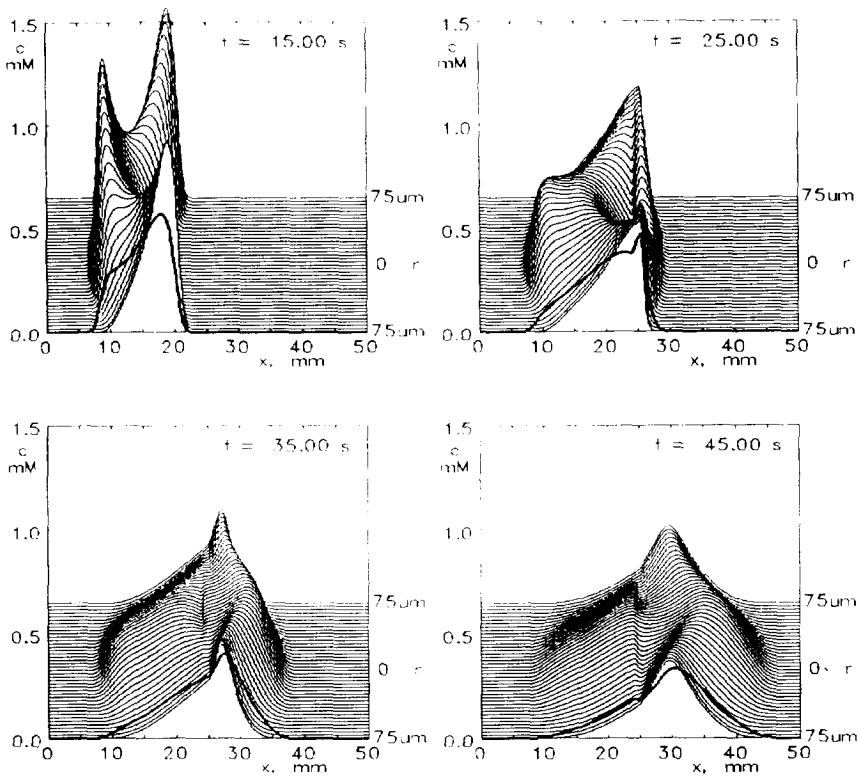

Fig. 2. Simulation of the peak profiles at various times t in a half-covered capillary column. Diffusion coefficient D, $5 \cdot 10^{-11}$ m^2 s^{-1}; radius of column a, $75 \cdot 10^{-6}$ m; length of column L, 0.05 m; electrophoretic velocity v_{ep}, 0. Thick line = mean axial concentration, c_m. (a) Axial and radial profiles of the peak; (b) time record of a detector located at $x = 0.03$ m.

signal of a detector at a given position. Hence, in Fig. 4d a time record of the mean concentration of the solute is presented for a time range large enough to enable the peak to pass the detector. The graph exhibits an asymmetric shape due to severe dispersion during its passage through the detector.

Finally, it should be realized that the widths of

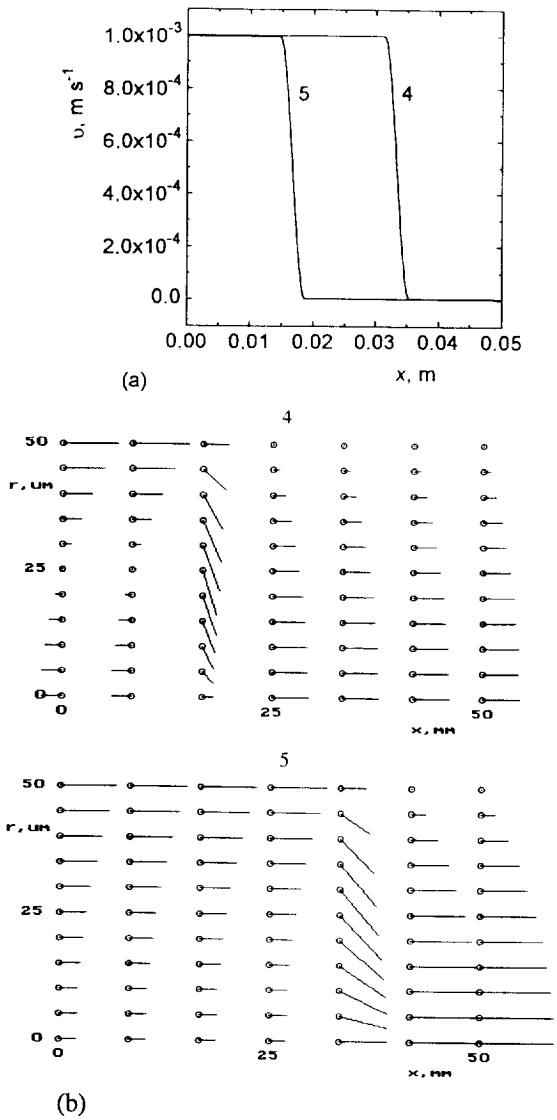

Fig. 3. Simulation of the stationary velocity field in a partly covered capillary column. Radius of column a, $50 \cdot 10^{-6}$ m; length of column L, 0.05 m; 4 and 5 = two different cases corresponding to two profiles of the electroosmotic velocity $v(x)$ at the column wall. (a) Boundary conditions; (b) velocity fields.

peaks in CZE are mostly much greater than the radius of the columns and, in the considered cases of a non-uniformly distributed zeta potential, the radial profile of the axial velocity is approximately parabolic. This brings the main contribution to the overall peak shape and its dispersion and, consequently, the well established theory of convective diffusion in laminar flow can be employed with good precision.

The contribution of the radial flow in transient regions and the convective terms are comparatively less significant. Nevertheless, many more extreme situations can be found where the use of the present model will be necessary.

5. Appendix

Here we derive Eq. 24, as we believe, in a simpler and more straightforward manner than in Ref. [9]. If non-linear terms in the Navier–Stokes equations are left out, the Stokes equations are obtained. Hence, by Eq. 3 the equation for the component v_x of the stationary solution $\vec{v}(x, r)$ of the Stokes equations is

$$0 = \nu \cdot \frac{\partial^2 v_x}{\partial x^2} + \nu \cdot \frac{1}{r} \cdot \frac{\partial}{\partial r}\left(r \cdot \frac{\partial v_x}{\partial r}\right) - \frac{1}{\rho} \cdot \frac{\partial p}{\partial x}$$

This equation is multiplied by r and integrated over any domain $x \in \langle 0, L \rangle$, $r \in \langle 0, \sigma \rangle$, $\sigma \in (0, a)$. By applying integration by parts and taking the boundary conditions into account, the first and third terms on the right-hand side are shown to be zero. Hence the relationship reduces to

$$\int_0^L \int_0^\sigma \frac{\partial}{\partial r}\left(r \cdot \frac{\partial v_x}{\partial r}\right) \mathrm{d}r \, \mathrm{d}x = 0$$

This provides

$$\sigma \int_0^L \frac{\partial v_x}{\partial r}(x, \sigma) \, \mathrm{d}x = 0$$

from which it is obtained immediately that the function $r \rightarrow \int_0^L v_x(x, r) \, \mathrm{d}x$ is constant in the interval $\langle 0, a \rangle$. Hence, according to the boundary condition Eq. 2, for every $r \in (0, a)$ it holds that

$$\int_0^L v_x(x, r) \, \mathrm{d}x = \int_0^L v(x) \, \mathrm{d}x$$

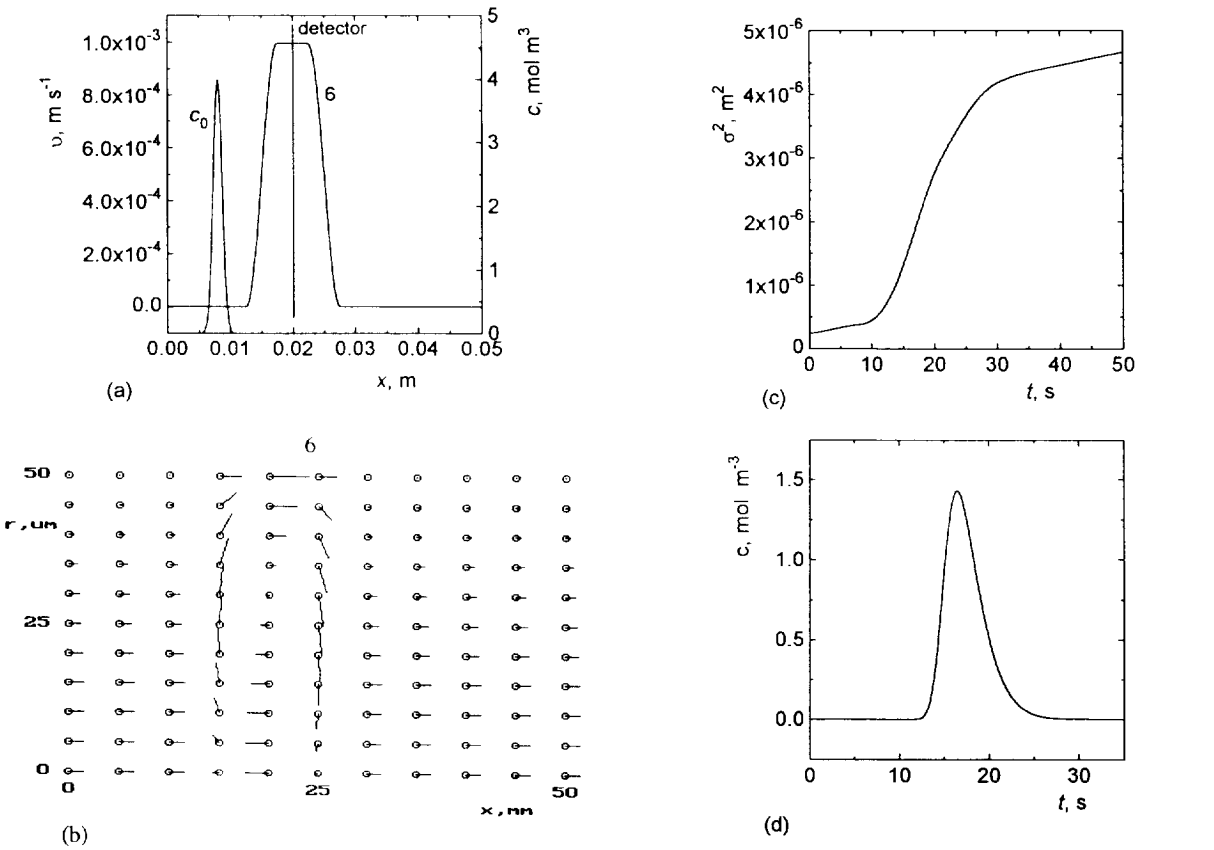

Fig. 4. Simulation of the stationary velocity field in a partly uncovered capillary column. Diffusion coefficient D, $2 \cdot 10^{-10}$ m^2 s^{-1}; radius of column a, $50 \cdot 10^{-6}$ m; length of column L, 0.05 m; electrophoretic velocity v_{ep}, 0.5 mm s^{-1}. c_0 = Initial condition, Eq. 35. 6 = Profile of the electroosmotic velocity $v(x)$ at the column wall. (a) Initial condition and boundary conditions; (b) velocity field; (c) simulated time-dependent variance; (d) time record of a detector located at $x = 0.02$ m.

From Eq. 5, it follows that the function $x \rightarrow \int_0^a v_x(x, r)r\ dr$ is constant on $(0, L)$. Hence,

$$v_m = \frac{2}{a^2}\int_0^a v_x(x, r)r\ dr$$

$$= \frac{2}{La^2}\int_0^L \int_0^a v_x(x, r)r\ dr\ dx$$

$$= \frac{2}{La^2}\int_0^L v(x)\ dx \int_0^a r\ dr$$

$$= \frac{1}{L}\int_0^L v(x)\ dx$$

The first and last terms form Eq. 24.

Acknowledgement

This work was supported by the Grant Agency of the Czech Republic, Grant Nos. 203/94/0698 and 203/93/0718.

References

[1] R.S. Berry, J.A. Rice and J. Rosse, Physical Chemistry, Wiley, New York, 1979.

[2] C.L. Rice and R.J. Whitehead, Phys. Chem., 69 (1965) 4017.

[3] M. Martin and G. Guiochon, Anal. Chem., 56 (1984) 614.

[4] M. Martin, G. Guiochon, Y. Walbroehl and J.V. Jorgenson, Anal. Chem., 57 (1985) 559.
[5] V.P. Andreev and E.E. Lisin, Electrophoresis, 13 (1992) 832.
[6] K.P. Tikhomolova, Electroosmosis, Ellis Horwood, New York, 1993.
[7] B. Gaš, M. Štědrý and E. Kenndler, J. Chromatogr., 709 (1995) 63.
[8] P. Chowdiah, D.T. Wasan and D. Didaspow, AICHE J., 27 (1981) 975.
[9] J.L. Anderson and W.K. Idol, Chem. Eng. Commun., 38 (1985) 93.
[10] R.L. Chien and J.C. Helmer, Anal. Chem., 63 (1991) 1354.
[11] J.T. Towns and F.E. Regnier, Anal. Chem., 64 (1992) 2473.
[12] C.L. Lee, W.C. Blanchard and C.T. Wu, Anal. Chem., 62 (1990) 1550.
[13] K. Ghowsi and R.J. Gale, J. Chromatogr., 559 (1991) 95.
[14] C.T. Wu, T.L. Huang, C.S. Lee and C.J. Miller, Anal. Chem., 65 (1993) 568.
[15] M.A. Hayes, I. Kheterpal and A.G. Ewing, Anal. Chem., 65 (1993) 2010.
[16] E.V. Dose and G.J. Guiochon, J. Chromatogr., 625 (1993) 263.
[17] T.J. Mueller, in H.J. Wirz and J.J. Smolderen (Editors), Numerical Methods in Fluid Dynamics, Hemisphere, 1978, Ch. 2.
[18] G. Taylor, Proc. R. Soc. London, Ser. A, 219 (1953) 186.
[19] G. Taylor, Proc. R. Soc. London, Ser. A, 225 (1954) 473.
[20] R. Aris, Proc. R. Soc. London, Ser. A, 235 (1956) 67.
[21] W.N. Gill, Proc. R. Soc. London, Ser. A, 298 (1967) 335.
[22] W.N. Gill and S. Sankarasubramanian, Proc. R. Soc. London, Ser. A, 316 (1970) 341.
[23] P.J. Roache, Computational Fluid Dynamics, Hermosa, Albuquerque, 1976.
[24] R. Peyret and T.D. Taylor, Computational Methods for Fluid Flow, Springer, New York, 1983.